

**Steric constraints control processing of glycosylphosphatidylinositol anchors in  
*Trypanosoma brucei***

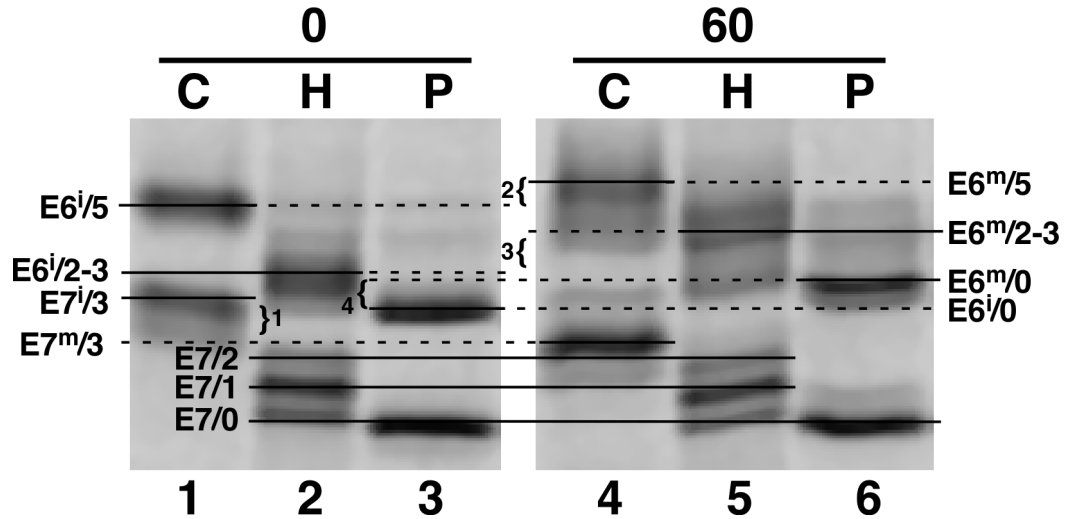
**Carolina M. Koeller<sup>1&</sup>, Calvin Tiengwe<sup>1&#</sup>, Kevin J. Schwartz<sup>2</sup> & James D. Bangs<sup>1\*</sup>**

From the <sup>1</sup>Department of Microbiology & Immunology, School of Medicine and Biomedical Sciences, University at Buffalo (SUNY), Buffalo, NY 14214, USA, and <sup>2</sup>Department of Medical Microbiology and Immunology, University of Wisconsin-Madison, Madison, Wisconsin, USA

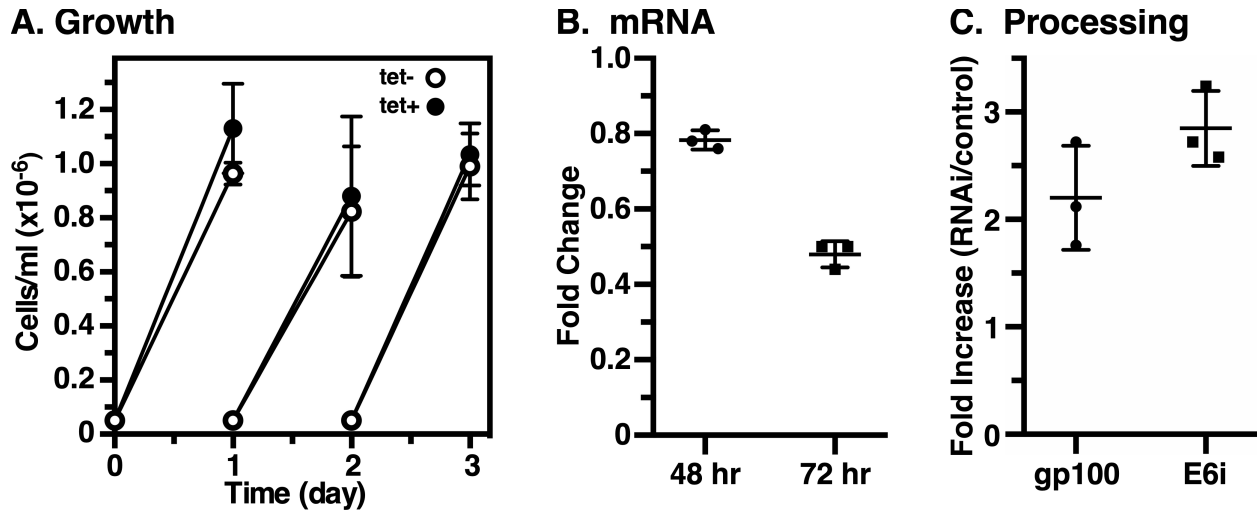
Supporting Information:      Figure S1

   Figure S2

   Figure S3



**Figure S1. Identification of glycoforms in de-N-glycosylated Tfr.** Phosphorimages from Fig. 2 are presented. Individual species are identified as E6 or E7 followed by immature (i) or mature (m) / # of N-glycans (0-5). Major shifts are: 1) Apparent decrease in size of fully glycosylated E7 from immature (lane 1, E7<sup>i</sup>/3) to mature (lane 4, E7<sup>m</sup>/3). We attribute this to trimming of N-glycans during cell transit (see also Fig. 3, lanes 4 & 10; Fig. 6, lanes 9 & 10). 2) Increase in size of fully glycosylated E6 from immature (lane 1, E6<sup>i</sup>/5) to mature (lane 4, E6<sup>m</sup>/5) glycoforms. This represents combined processing of paucimannose N-glycans and the GPI glycan core. 3) Increase in size of partially de-N-glycosylated (Endo H treatment) E6 from immature (lane 2, E6<sup>i</sup>/2-3) to mature (lane 5, E6<sup>m</sup>/2-3) glycoforms. This represents combined processing of paucimannose N-glycans and the GPI glycan. 4) Increase in size of fully de-N-glycosylated (PNGase F treatment) E6 from immature (lane 3, E6<sup>i</sup>/0) to mature (lane 6, E6<sup>m</sup>/0). This represents processing of the GPI glycan core.



**Figure S2. TbSTT3A knock down.** **A.** The TbSTT3A RNAi cell line was cultured without (tet-) or with (tet+) tetracycline to initiate specific dsRNA synthesis. Cell density was monitored by microscopic counting, and cultures were adjusted to starting densities every day. Data presented as means  $\pm$  std. dev. (n=3). **B.** TbSTT3A mRNA was quantified by qRT-PCR at the indicated times post induction (means  $\pm$  std. dev., n=3). Signals are normalized to uninduced cells at each time point. **C.** The signals for gp100 and E6i in Fig. 4 and two identical biological replicates were quantified by phosphorimaging (means  $\pm$  std. dev., n=3). In each case the signals of control (tet-, lanes 1 & 4) and silenced (tet+, lanes 7 & 10) were averaged as technical replicates within each experiment. The data are graphed as fold increase (tet+/tet-).

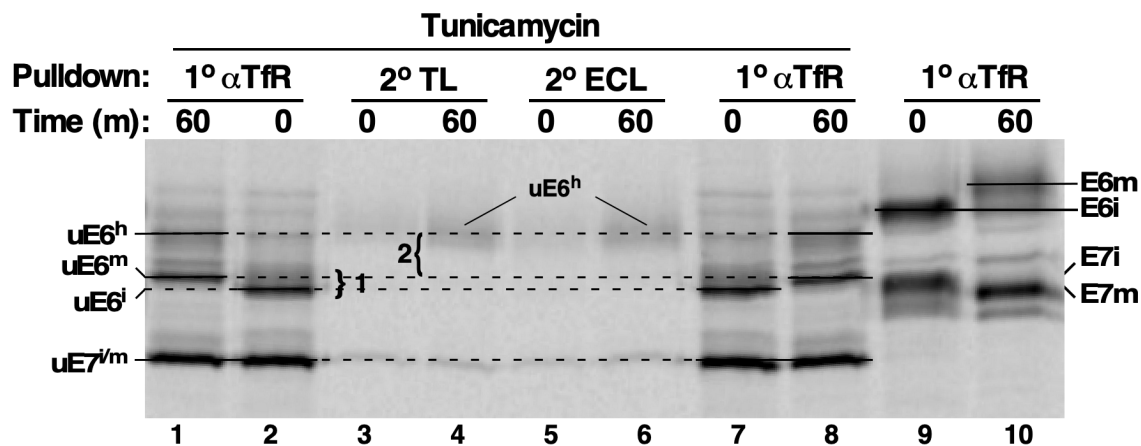


**Figure S3. Identification of glycoforms in un-N-glycosylated TfR.** The phosphorimage from Fig. 7 is presented. Individual species are identified as E6 or E7 followed by immature (i) or mature (m). Un-N-glycosylated species are indicated by the prefix 'u'. Major shifts are: 1) Increase in size of un-N-glycosylated E6 from immature (uE6<sup>i</sup>, lanes 2 & 7) to mature (uE6<sup>m</sup>, lanes 1 & 8) glycoforms. This represents processing of the GPI glycan in the absence of N-glycans. 2) Increase in size of un-N-glycosylated E6 from mature (uE6<sup>m</sup>, lanes 1 & 8) to the TL- and ELC-reactive hypermodified (uE6<sup>h</sup>, lanes 4 & 6) glycoform. We presume that this represents extensive modification of a subset of mature un-N-glycosylated E6 by addition of poly-N-acetylglucosamine to the GPI glycan.